INTEGRATING MULTIPLE DATASETS TO ALIGN BIOLOGICAL AND STATISTICAL POPULATIONS FOR ABUNDANCE ESTIMATION

Michelle L. Kissling, Wildlife Biology Program, University of Montana, Missoula, Montana, USA, 59812; corresponding author: kissling.michelle@gmail.com

Paul M. Lukacs, Wildlife Biology Program, University of Montana, Missoula, Montana, USA, 59812

Kelly Nesvacil, U.S. Fish and Wildlife Service, Corpus Christi, Texas, USA, 78411

Scott M. Gende, National Park Service, Juneau, Alaska, USA, 99801

Grey W. Pendleton, Alaska Department of Fish and Game, Juneau, Alaska, USA, 99801

ABSTRACT

Ideally, a statistical population is the same as, or accurately represents its corresponding biological population. However, in practice, they rarely align in space and time, which can lead to variable exposure to sampling and biased inference. We often view a population mismatch as a temporary emigration process and resolve it with replicate and/or repeat sampling, though this approach is not feasible for all species and habitats. We developed a hierarchical Bayesian integrated model to estimate abundance of a biological population of the Kittlitz's murrelet (*Brachyramphus brevirostris*), a highly mobile, non-territorial, ice-associated seabird of conservation concern in Alaska and eastern Russia. Our model combines datasets from boat and telemetry surveys to account for all components of detection probability, specifically using telemetry locations to estimate probability of presence (p_p) and line transect distance sampling to estimate probability of detection (p_d). By estimating p_p directly, we were able to account for temporary emigration from the sampled area, which changed with shifting icefloes between sampling occasions. Between 2007 and 2012, annual p_p was highly variable, ranging from 0.33 to 0.75 (median=0.50, SE=0.02), but was not predictable using five environmental covariates. In years when two boat surveys were conducted, our model reduced the coefficient of variation (CV) of abundance estimates by 13–35%, yet in the year with only one boat survey (2009), the CV skyrocketed about 10-fold, emphasizing the importance of a second survey if p_p varies. Although we increased the precision of annual abundance estimates by accounting for p_p, we did not see the same improvement in the estimate of mean *r*, or trend, indicating that while we reduced within-year variance, we failed to account for a source(s) of variation across years, which we suspect is related to the propensity for murrelets to skip breeding in some years. Our integrated model to resolve a population mismatch is simple, flexible, and scalable for generating unbiased and precise abundance estimates of highly mobile species that occupy dynamic habitats where other open population models are not feasible. Importantly, it improves inference of the biological population, which is the true population of interest. We urge ecologists to think critically about the population in which they want to draw inference, especially as tracking technology improves and model complexity increases.

KEYWORDS

temporary emigration, biological population, statistical population, integrated model, detection probability, seabird, *Brachyramphus* murrelet, superpopulation

INTRODUCTION

The population concept is a central theme in ecology, management, and conservation. Yet, the term 'population' has many definitions depending on the underlying objectives and the context in which it is used (Waples and Gaggiotti 2006, Hammond et al. 2021). Fundamentally, we can distinguish between two types of populations: biological and statistical. A biological population is a group of individuals that share some attributes with ecological or evolutionary meaning. In contrast, a statistical population describes an aggregate of things, which may or may not be individuals, about which we draw inference, usually by sampling. While many variations of these two types of populations exist, such as sampled and target (Cochran 1977), natural and local (Andrewartha and Birch 1954), and resource and statistical (Reynolds 2012), the distinguishing principle across them is the same: one population is what we really want to know something about (biological) and the other is what we use to infer what we want to know (statistical).

Ideally, a statistical population is the same as, or accurately represents its corresponding biological population (Cochran 1977). However, in practice, they rarely align in space and time, which can lead to variable exposure to sampling and biased inference about the population of interest. Although statistical inference can be appropriately drawn from the sample, it only extends to the statistical population, as defined by the researcher. In contrast, scientific inference, which is a far broader concept that is based on evidence and reasoning, applies to the biological population. The crucial distinction between scientific and statistical inference in population ecology studies is often overlooked, especially with the increasing use of complex models, in part because of the challenges in delineating a biological population (Berryman 2002, Camus and Lima 2002). Yet, because scientific inference is the knowledge goal of these studies, any misalignment between the statistical and biological populations can be problematic and misleading if left unresolved.

Generally, a population mismatch can occur for two primary reasons. First, one can arise when knowledge about the biological population is limited. Often researchers design investigations before having a clear understanding of the variation in the spatial and temporal dynamics of the population of interest, potentially and unknowingly leading to a mismatch. Second, a mismatch can occur when the distribution of the biological population across space and time is known but access is restricted, which can result in a poor sampling design. This situation, which is termed a frame error (Reynolds 2012), can arise for physical (e.g., natural barriers), logistical (e.g., cost, safety), legal (e.g., landownership boundaries), and political (e.g., international borders) reasons.

For mobile organisms, we often view a population mismatch as a form of temporary emigration, whereby individuals are temporarily not exposed to sampling for a variety of potential reasons (Kendall et al. 1997). It is an oddly vague process with biological and statistical drivers that usually are confounded. For example, individuals may temporarily emigrate for biological reasons like searching for food or avoiding predation, statistical reasons such as unequal sampling probability owing to a frame error, or a combination of both. Ultimately, temporary emigration is a detection issue. If it occurs randomly, temporary emigration will inflate

unexplained variance and reduce precision of abundance estimates; if it occurs non-randomly, i.e., with a temporal trend, it will bias estimates.

Fortunately, over the last few decades, many analytical approaches have been developed to account for temporary emigration when estimating abundance. The most notable methods are capture-recapture models that use robust design (Kendall et al. 1997) or are spatially explicit (Royle and Young 2008), extensions of N-mixture models (e.g., Chandler et al. 2011), thinned point process models (e.g., Mizel et al. 2018), and models that combine methodology (e.g., Powell et al. 2000, Amundson et al. 2014). These approaches use spatial and temporal replicates with short periods of closure (hereafter replicate sampling) or the ability to identify individuals during sampling (hereafter repeat sampling) to estimate temporary emigration and abundance of the biological population, sometimes referred to in this context as the superpopulation (Schwarz and Arnason 1996). While these models are flexible and powerful, they are not feasible for all species and habitats, or in all situations.

Some species and habitats are too complex to obtain a sufficient number of replicate or repeat samples across space or time. Species that are difficult to recapture or resight during sampling are inherently unsuitable for capture-recapture methods, as reliable models cannot be developed with few observations. Further, highly mobile, non-territorial species, such as many marine species, cannot satisfy the closure assumption, even for short periods, unless the study area is large relative to movement, which paradoxically often makes sufficient sampling impractical. The same principle applies to species that are sampled during non-territorial portions of their life cycle, such as winter concentrations of ungulates or migrating raptors, when individuals are not tied to a particular area (e.g., breeding site). Finally, dynamic habitats that can change between sampling occasions (e.g., drift ice), are not conducive to replicate sampling; not only can the size and shape of the sampled area vary, but also the individuals exposed to sampling.

An alternative approach to handling a population mismatch that does not require replicate or repeat sampling is to decompose the detection process. Nichols et al. (2009) described four components of overall detection (p): (1) probability that the individual's home range includes at least a portion of the sample area (p_s); (2) probability of presence within the sample area during a survey (p_p); (3) probability of availability given presence (p_a); and (4) probability of detection given presence and availability (p_d). The first component (p_s) simply confirms that an individual is a member of the biological population, and the last component (p_d) refers to the actual observation process, that is whether an individual was observed. Jointly, the second and third components (p_p and p_a, respectively) describe temporary emigration, with the second component (p_p) being spatial temporary emigration and specifically addressing the population mismatch issue, and the third component (p_a) as random temporary emigration (Kery and Royle 2016). A major advantage to using this approach is that each component can be estimated separately using different datasets and even different data types (Hostetter et al. 2019), making it suitable for all species and habitats provided that the components are estimable.

We applied this approach to resolve a population mismatch for the Kittlitz's murrelet (*Brachyramphus brevirostris*), a highly mobile, non-territorial, ice-associated seabird that is irregularly distributed across coastal Alaska and eastern Russia. Several aspects of this species' life history complicate methods that rely on replicate or repeat sampling to estimate spatial

temporary emigration. Unlike most seabirds, Kittlitz's murrelets do not nest in colonies, but instead nest solitarily at low densities, usually in remote inaccessible locations (Kissling et al. 2015a). Thus, populations cannot be monitored at colonies like most seabirds where replicate and repeat sampling is practical and efficient. Additionally, owing to the small size, cryptic behavior, and prevalence of nonbreeding in this species, capture-recapture and resight models are not feasible. It is nearly impossible to resight banded or marked murrelets on the water or in flight and recapture rates are too low to be useful for estimating abundance (Kissling et al. 2015b), in part because of challenges with nighttime captures during summer at high latitudes.

Instead, the only viable way to monitor Kittlitz's murrelet populations is with boat-based abundance surveys that are conducted during the breeding season when most murrelets concentrate in bays and fjords often near tidewater glaciers (Day et al. 2020). A design challenge and safety concern for these surveys is the presence of icefloes, large tidal fluctuations, glacial river debris, and the possibility of rough seas. These dynamic conditions can restrict boat access to portions of the study area and cause murrelets to redistribute over short time intervals, resulting in a population mismatch that cannot be handled with replicate sampling, as neither the murrelets nor the habitat can meet the closure assumption.

We developed a hierarchical Bayesian integrated model to estimate abundance of a biological population of the Kittlitz's murrelet in a dynamic environment. Our model combines datasets from telemetry flights to locate radio-tagged murrelets, boat-based distance sampling surveys, and dive behavior trials to account for all components of detection probability (p_s, p_p, p_a, p_d). Our primary objective was to develop an analytical tool to align the statistical and biological populations of this unusual species so that we could generate unbiased abundance estimates for later use in an integrated population model. More specifically, here, we aimed to (1) estimate detection probability components and their variation; (2) assess predictability of p_p using environmental covariates; and (3) estimate abundance and trend of the statistical (without p_p) and biological populations (with p_p) and identify any sources of bias. We also wanted to assess whether we delineated the biological population of Kittlitz's murrelets in our study area appropriately.

STUDY AREA

Our study was centered in Icy Bay, Alaska, USA, located in the northeastern Gulf of Alaska and ~110 kilometers northwest of the town of Yakutat (Figure 1). Icy Bay is a highly dynamic glacial fjord system that has experienced multiple, rapid ice advances and subsequent retreats over the past ~3,800 years with the most recent retreat of approximately 40 km during the 20th century (Barclay et al. 2006).

Currently, Icy Bay comprises a shallow outer bay and a deeper inner bay. The outer bay is adjacent to the Gulf of Alaska and measures 6 km wide at the mouth. The inner bay is divided into four distinct fjords with each terminating at an active tidewater glacier. The Guyot, Yahtse, and Tsaa glaciers are one glacial system, while the Tyndall Glacier in Taan Fjord is an independent system. The Malaspina Glacier, the largest piedmont glacier in North America, is situated to the east and empties meltwater and glacial sediment into Icy Bay via the Caetani River system. Gull Island, near the mouth of the Caetani River, provides a catchment for glacial sediment circulating in the bay and therefore the size and shape of the island, as well as the water

depths adjacent to the island, vary within and across years. Currently, at extremely low tides (<0.5 m), Gull Island is connected to the mainland by a thin, sandy strip of beach and at extremely high tides (>3.0 m), the waters are deep enough that the island can be circumnavigated in a boat with an outboard engine. There are two small bays within Icy Bay (Riou and Moraine bays) that have submerged marine sills at their mouths making it difficult to access these small bays during low tides. The total surface of Icy Bay is approximately 263 km^2, but typically the upper half of the bay is covered in thick ice floes and large icebergs, resulting in an open water surface area of ~160 km^2 with considerable variability within and across years depending on glacial calving activity.

METHODS

Data collection

Boat surveys.— From 2005 to 2017, we conducted two boat-based abundance surveys between 1 and 15 July in each of eight years (2005, 2007–2008, 2010–2012, 2016–2017) and one survey on 17 July 2009. The target sampling area was ~160 km^2, consisting of the Main Bay and Taan Fjord (Figure 1). Generally, we completed surveys in a single day, though rarely it took two days, depending on tides and other logistical factors. Boat surveys involved line transect distance sampling, following the protocol described in Kissling et al. (2007, 2011), with one exception; in 2016 and 2017, we estimated the angle and distance from the boat to each murrelet group as opposed to estimating perpendicular distance from the line transect (all other years). We also recorded group size, behavior (water, flying), and foraging activity of all *Brachyramphus* murrelets observed. Both Kittlitz's and its congeneric marbled murrelet (*B. marmoratus*) occur in Icy Bay and can be difficult to distinguish, especially at a distance; if an observer was unable to identify a murrelet (or group of murrelets) to species, it was recorded as an unidentified murrelet(s).

Telemetry surveys.— We captured Kittlitz's Murrelets on the water using the night-lighting method (Whitworth et al. 1997) in and near Icy Bay between 8 May and 3 June, 2007–2012. Following capture, we transported murrelets to a larger vessel for processing, which included morphometric measurements, blood sampling for sex identification, and banding. We deployed very-high-frequency (VHF) radio transmitters on a subset of after-second-year murrelets captured each year. We attached the transmitters (Advanced Telemetry Systems, Inc., Isanti, Minnesota [ATS]; model number A4360) using a subcutaneous anchor on the bird's back between the scapulars (Newman et al. 1999). If both birds of a pair were captured, we randomly selected one bird to radio-tag to ensure independence. We released murrelets immediately after processing was complete.

We attempted to locate radio-tagged murrelets 2–5 times per week for at least eight weeks after tagging using fixed-wing aircraft equipped with "H-style" antennas mounted on the struts. We were not able to search for tagged birds using a strict design, but instead aimed for complete coverage of the study area in a systematic way that allowed for safe flying. We first attempted to locate all murrelets on the water in and near Icy Bay within gliding distance of shore; if murrelets were not detected at sea, we flew over all assumed potential nesting habitat within reason (e.g., fuel constraints) to locate incubating birds. We conducted telemetry flights on the same day as boat surveys; on occasion, we had to fly the telemetry survey on the following day

because of aircraft availability. All telemetry flights were completed in less than four hours. For more details on capture, handling, tagging, and relocating see Kissling et al. (2015a, b, 2016).

During each flight, we mapped ice conditions into five categories of increasing ice density: none, brash ice, open pack ice, close pack ice, and very close pack ice. We defined brash ice as accumulations of floating ice made up of fragments not more than 2 m across, open pack ice as low concentration pack ice with many leads and polynyas and the floes generally were not in contact, close pack ice as moderate concentration pack ice with the floes generally in contact, and very close pack ice as high concentration pack ice with very little water visible (Bowditch classification; NOAA 2007). Following each flight, we digitized these maps in ArcGIS (ESRI, v10.7.1) and estimated ice cover (km^2) by category in the study area on that day. We then assigned all locations of radio-tagged murrelets to an ice category using the ice condition maps for each corresponding telemetry flight.

We compiled environmental data for murrelets located during telemetry flights. Using the date and time of each location, we determined tidal stage, which represented the vertical movement of water, as ebb or flood, and tidal current strength, the horizontal movement of water, following Kissling et al. (2007). We also acquired the daily precipitation (mm), which affected freshwater input volume and turbidity, and average daily wind speed (m/sec), which influenced icefloe movement and ocean surface conditions, from a weather station in Icy Bay (https://www.ncdc.noaa.gov/cdo-web/). Lastly, we calculated the proportion of the Icy Bay state (i.e., the area sampled during boat surveys; see below) that was covered in ice (all categories) on the flight day.

Data analysis

Components of detection probability.—We considered detection probability components individually, which allowed for use of different datasets, and then combined those necessary in an integrated model (see below). This approach was efficient, as two components of detection probability, p_s and p_a, were deemed to be close to 1 and unnecessary in the integrated model.

We determined that p_s, the probability that an individual could be included in the sampled area during a boat survey, was 1 in all years by examining both home ranges (95% utilization distribution [UD]) and core use areas (50% UD) of radio-tagged murrelets (Kissling 2023). Therefore, we did not include p_s in our integrated model.

We estimated p_p, the probability that an individual was present in the sampled area during a boat survey, using location data from radio-tagged murrelets. Following Kissling et al. (2015b), we assigned each telemetry location to one of five spatial states (Figure 1): Icy Bay, which comprised Main Bay and Taan Fjord sub-states and was the core area sampled by boat; East Bay, which was too shallow for a boat; Upper Bay, which was too icy; Ocean, which was too rough; or at a nest. Any telemetry locations outside of these five states were removed from our analysis (<2% of all locations); notably, none of these individuals were located again. We then merged data on spatial state and ice category for each telemetry location. We considered a radio-tagged murrelet to be present in the sampled area if it was in Icy Bay state and in ice categories of none, brash ice, or open pack ice, where we could conduct boat surveys safely. If a radio-tagged

murrelet was at a nest or in the East Bay, Upper Bay, Ocean, or in close pack ice or very close pack ice, it was deemed not present.

To estimate p_p, we filtered telemetry data to include locations from 1 to 15 July to overlap with our boat survey protocol. We explored the use of telemetry locations acquired in 1-, 3-, 5-, and 7-day windows surrounding the boat survey; for example, if a boat survey was conducted on 8 July, the 3-day window was 7–9 July and the 5-day window was 6–10 July. All telemetry locations collected during a specific window were used to estimate a single value of p_p. In 2009, we conducted a single boat survey late (17 July) because of boat availability and poor weather and therefore, we shifted the windows to center on the later date. In all years, we found that p_p varied little with window length, though precision improved (Appendix 1), which was unsurprising given that sample size increased (i.e., number of telemetry locations). Here, we report results for the 3-day window only because it was the best tradeoff between improved precision while maintaining a short temporal window around each survey. For comparison, we also report p_p for the entire 15-day period (1–15 July).

We conducted boat-based dive behavior trials to estimate p_a, the probability that a murrelet was available for detection (i.e., not underwater) given presence. We determined that the probability of a murrelet being unavailable for detection was quite low (0.032 ± 0.007; see details in Lukacs et al. 2010). Therefore, we assumed p_a was close enough to 1 not to affect abundance estimates, and, like p_s, did not include it in our integrated model.

Finally, we estimated p_d, or the probability of being detected given presence and availability on boat surveys, using conventional distance sampling. We filtered data to include murrelets observed on the water only, i.e., we excluded flying birds from our analysis. We pooled data across both surveys each year (except 2009) and all *Brachyramphus* murrelets to estimate p_d because observers rarely changed, and we did not expect detection probability to be different by species. We then truncated the upper 5% of distance data. We examined the effect of group size on the scale parameter of the half normal detection function, but it had no effect in any year (based on ΔAIC values and Cramer-von Mises tests) and therefore, we did not include group size in our analyses.

To allocate murrelets not identified to species (i.e., unidentified *Brachyramphus* murrelets) during boat surveys, we estimated the probability of being a Kittlitz's murrelet (p_k), as opposed to a marbled murrelet, in two strata (m) in Icy Bay (Figure 1). While Kittlitz's murrelets are uniformly distributed throughout the bay, marbled murrelets are not; they are rarely located in Taan Fjord (Kissling et al. 2007, 2011). Therefore, we divided our sampling area into two strata, Main Bay and Taan Fjord, to satisfy the assumption of uniform distribution when estimating p_k. Note that these strata were the same as the Main Bay and Taan Fjord sub-states described for p_p; we used different terminology to avoid confusion in the code (Appendix 4).

Integrated model for biological population abundance.—We developed a hierarchical Bayesian integrated model to estimate annual abundance of the biological population. We used data augmentation to represent a relatively large number of potential but unobserved groups in our sampling area during each boat survey (Royle and Dorazio 2008). To estimate a single value for annual abundance, we used the following joint likelihood:

$$L[M \mid data] = \left[L[M|N_i, p_{p,i}]\right] \left[L\left(p_{p,i} \mid y_{p_{p,i}}\right)\right] \left[L(p_{d,\cdot}|y_{p_{d,\cdot}})\right] \left[L(p_{k,\cdot m}|y_{p_{k,\cdot m}})\right]$$

where M is the abundance of the biological population, N_i is the statistical population abundance estimated for survey i, $p_{p,i}$ is the probability of presence for survey i, $p_{d,\cdot}$ is the probability of detection across both surveys, $p_{k,\cdot m}$ is the probability of being a Kittlitz's murrelet across both surveys by strata m, and *data* refers to the boat and telemetry survey data.

We modeled $p_{p,i}$ on the logit scale as

$$y_{p_{p,ij}} \sim Bernoulli(p_{p,ij}),$$

where individual locations (j) during each survey (i) were used to estimate $p_{p,ij}$. We did not include covariates in this sub-model because we did not identify any that helped explain variation in $p_{p,ij}$ (see 'Predicting probability of presence' below).

We modeled $p_{d,\cdot}$ on the log scale using the perpendicular distance of each group q from the transect line (x_{iq}) and the half-normal detection function:

$$p_{d,\cdot q} = exp\left(-\frac{x_{iq}^2}{2\sigma_{iq}^2}\right),$$

where σ_{iq} is the scale parameter. As noted above, we did not include group size as a covariate on σ_{iq} because it did not help explain variation in $p_{d,\cdot}$. We estimated the probability of being a Kittlitz's murrelet as

$$y_{p_{k,\cdot m}} \sim Bernoulli(p_{k,\cdot m}),$$

where identified groups in each stratum across all surveys were used to estimate $p_{k,\cdot m}$. We modeled group size of the augmented groups as

$$y_{g,\cdot q} \sim Poisson(\lambda),$$

where $y_{g,\cdot q}$ is the observed group size q across all surveys and λ is mean group size.

Predicting probability of presence.—We attempted to predict p_p of radio-tagged murrelets in the sampling area using environmental covariates so that we could estimate it in years for which we lacked telemetry data (i.e. 2005, 2016, and 2017) and potentially improve our boat survey protocol to minimize variation in p_p in the future. We considered five covariates: tidal stage, tidal current strength, daily precipitation, daily average wind speed, and the proportion of Icy Bay state covered in ice. We hypothesized that p_p would be higher during the flood (incoming tide) than the ebb and positively associated with tidal current strength, reasoning that these conditions would concentrate murrelet prey. We posited that p_p would be negatively associated with daily precipitation because of increased freshwater input into Icy Bay, possibly reducing prey or access to prey because of higher turbidity, and positively related to daily average wind speed, as

an indicator of offshore storms. Lastly, we hypothesized that p_p would be inversely related to the proportion of ice in the Icy Bay state, as ice would displace murrelets.

We used a generalized linear mixed model (binomial error, logit link) with random effects for year and individual to explore our ability to predict p_p with environmental covariates. We filtered telemetry data to include the same dates as our boat survey protocol (1–15 July); we also excluded murrelet locations at a nest because environmental data for those records were not relevant. We scaled all covariates to have a mean of 0 and standard deviation of 1. To assess our model, we used cross-validation by randomly selecting 80% of the records to estimate p_p, then using the estimated p_p to predict presence for the remaining 20%, setting a threshold of 0.5 to denote whether a murrelet was predicted to be present or not in the sampling area. We then created a confusion matrix comparing predicted and actual presence to evaluate our ability to predict presence.

Estimating trend in abundance.—We used a state space model to estimate trend in abundance, or the instantaneous growth rate (r), of the statistical and biological populations (i.e. without and with p_p, respectively). Our state space model included a random effect for year and weighted the response variable (log abundance) by the inverse of its variance. For years with direct estimates of p_p (2007–2012), we used abundance of the biological population estimated incorporating telemetry data (3-day window). In years without telemetry data (2005, 2016–2017), we used mean p_p from across the 15-day period in all years, with year and individual included as random effects in the estimation process. We intended to predict p_p for use in these non-telemetry years, but because our predictive power was low, we opted to use mean p_p. To assess the effect of including p_p in our trend estimate, we examined the root-mean-square-error (RMSE) of mean r and percent change of coefficients of variation (CV) of lambda (λ), converted from mean r to avoid division by 0, between models without and with p_p. We report trend results across all years (2005–2017).

We fit all models using JAGS (Plummer 2003) with R 4.2.1 (R Core Team 2019) using R2jags as an interface. We used weakly informative priors on all parameters and 3 chains of 50,000 iterations, discarding the first 15,000 per chain as burn-in (Appendix 4). We assessed model convergence through visual inspection of trace plots and the Gelman-Rubin diagnostic (Brooks and Gelman 1998). We assumed convergence had occurred when chains overlapped substantially, and the Gelman-Rubin diagnostic was <1.1 for all parameters.

RESULTS

Components of detection probability

We radio-tagged 191 Kittlitz's murrelets between 12 May and 3 June, 2007–2012. Of these, 132 birds remained alive in the study area until at least 1 July when boat surveys commenced, contributing to 516 telemetry locations that were used to estimate p_p (Table 1). Across all flights and years, relocations of most radio-tagged murrelets were in the Icy Bay state (53%) where boat surveys occurred, followed by the inaccessible states of Ocean (24%), East Bay (18%), Nest (4%), and Upper Bay (<1%; Appendix 3a). Only 5% of murrelets in the Icy Bay state were in close pack ice; the remainder were in open pack ice (8%), brash ice (15%), or no ice (72%; Appendix 3b).

Across all years, the median of p_p was 0.50 (SE=0.02). During the 15-day period in which boat surveys were conducted, median annual estimates of p_p ranged from 0.35 (SE=0.06) to 0.65 (SE=0.04; Figure 2a), which was similar to median estimates from the 3-day window surrounding each survey (0.32 [SE=0.10]–0.76 [SE=0.09]; Appendix 1). Within a year, p_p varied little, as indicated by the points falling close to the identity line (Figure 3). Although the 95% credible intervals (CrI) across surveys and within a year always overlapped, they narrowed as the window widened, reflecting an increase in the number of telemetry locations used to estimate p_p (Appendix 1).

Our ability to predict p_p using five environmental covariates was generally poor (Figure 4). We correctly predicted 62% of the observed outcomes and incorrectly predicted 38%. Of the environmental covariates examined, proportion of Icy Bay state covered in ice was the only one with 95% CrI that did not include 0 (β_{ice} = -0.356, CrI = -0.665, -0.059). While our hypothesis that p_p would be higher during a flood tide was not supported (β_{tide} = -0.006, CrI = -0.345, 0.356), we found that p_p was more variable with a flood compared to an ebb tide (Figure 4b).

Between 2005 and 2017, we conducted 17 boat surveys for *Brachyramphus* murrelets, of which only one covered the sampling area completely (mean fraction of sampling area covered=0.80, range=0.56–1.00; Table 1). This limitation of boat survey coverage due to shifting ice underscores the dynamic nature of our study area. Median annual estimates of p_d varied from 0.49 to 0.77 with CVs below 9% (Figure 2b). The probability that a detected *Brachyramphus* murrelet was a Kittlitz's murrelet, not a marbled murrelet, was high in both spatial strata, but lower and more variable in the Main Bay (range=0.72–1.00) compared to Taan Fjord (range=0.95–1.00; Figure 2c,d).

Abundance and trend

Abundance estimates of the statistical population were positively correlated with estimates of p_p; that is, when p_p was low, abundance was low, and vice versa (Figure 5), suggesting that Kittlitz's murrelets in Icy Bay were functioning as a single biological population. In all years, biological population abundance estimates were generally stable across all window lengths (Appendix 2). In years when two boat surveys were conducted, our integrated model with p_p reduced CVs of annual abundance estimates by 13–35%; in the year with only one boat survey (2009), CVs increased by 270% (Figure 6), likely because the CV of the 2009 population estimate was highly underestimated.

From 2005 to 2017, the trends in abundance of the statistical and biological populations were negative (Figure 7). The probability of a decline (mean $r < 0$) across our study area was 67% for the statistical population and 73% for the biological population. Estimates of mean r were -0.024 (CrI = -0.231, 0.183) for the statistical population (i.e., without p_p) and -0.043 (CrI = -0.265, 0.191) for the biological population (i.e., with p_p). By including p_p in the state space model, we reduced sampling variance in the estimate of mean r by 17%. However, the CV for λ increased by 12% and the RMSE for mean r increased from 0.160 to 0.185, indicating that we reduced within-year variance by accounting for p_p, but not across-year variance.

DISCUSSION

We developed a contemporary integrated model to resolve a population mismatch and generate unbiased abundance estimates of a highly mobile, non-territorial species, the Kittlitz's murrelet, in a dynamic marine environment. By decomposing detection probability, we were able to use multiple datasets of different data types that did not rely on replicate or repeat sampling, which was not feasible for our study species or area without an unrealistically large number of sampling occasions or sites (e.g., N-mixture models; Royle 2004, Barker et al. 2008, Hostetter et al. 2019). Alternatively, we would have needed to devise a way to increase capture probabilities to utilize capture-recapture or resight models effectively (Burnham et al. 1987). Moreover, the hierarchical structure of our integrated model allowed us to work within a single analytical framework and appropriately account for all sources of uncertainty.

We are not aware of another abundance model that accounts for all components of detection probability, especially p_p, without using replicate or repeat sampling methods. Fischbach et al. (2022) developed a similar integrated model to account for haulout probability, which is analogous to p_p, for estimating abundance of Pacific walrus (*Odobenus rosmarus divergens*), a species like *Brachyramphus* murrelets for which population monitoring is notoriously difficult. Their model combined count data from unoccupied aircraft systems and telemetry data, and therefore, while conceptually similar to our model, it is not applicable to our situation because of differences in data types and habitat dynamics, nor does it account for p_a or p_d. In these ways, our model builds on that of Fischbach et al. (2022) and adds to the toolbox of demographic models that account for spatial temporary emigration.

By accounting for p_p in our model, we improved the precision of annual abundance estimates by 13–35% when we followed our standard protocol of conducting two boat surveys. However, results from 2009, when only one boat survey was conducted, clearly indicated that p_p and survey effort were conflated, as the CV for the abundance estimate increased about tenfold. This outcome emphasizes the importance of a second boat survey annually if p_p varies; otherwise, the abundance estimate from a single survey can have misleadingly high precision. We suspect this implication would be true for other highly mobile species and dynamic systems as well. Nonetheless, our ability to notably improve CVs for abundance estimates is a major achievement for a species often plagued with imprecise estimates (USFWS 2013, Hoekman 2019).

Although we increased the precision of annual abundance estimates, we did not see the same improvement in the estimate of mean r, or trend. Thus, while we explained and reduced variation in abundance within a year, we failed to account for a source(s) of variation across years. We suspect it relates to the propensity for Kittlitz's murrelets to skip breeding in some years and resultant variable return rates to Icy Bay. A modeling exercise such as a life-stage simulation analysis (Wisdom et al. 2000) or an integrated population model (Schaub et al. 2007) would help approximate the potential influence of these latent parameters until direct data are available. It is worth noting that while we did not increase precision of the trend estimate, we also did not reduce it even though we added a parameter to the estimation process, suggesting some information about p_p was useful.

Though a population mismatch existed, we found that abundance estimates for the statistical population of Kittlitz's murrelets in Icy Bay were proportional to those of the biological population. We were somewhat surprised by this finding because, based on a survival analysis

with the same telemetry dataset, radio-tagged murrelets moved frequently among spatial states with daily transition probabilities ranging from 0.135 to 0.279 (Kissling et al. 2015b). Yet, despite these moderate movement rates, p_p varied little within a year (Figure 3). Further, p_p was correlated with abundance of the statistical population across years (Figure 5), which suggests that murrelets in our study area were operating as a single biological population, otherwise we would have expected discordance. Importantly, we did not detect a temporal trend in p_p, the link between the two types of populations, meaning that p_p in the statistical population was random with respect to the biological population and inference could be extended without bias.

As with all models, our model has assumptions beyond those associated with specific methods like radio telemetry (White and Garrott 1990) and distance sampling (Buckland et al. 2001). Inherent to boat and telemetry surveys, we assumed that the statistical population was closed with respect to p_p for survey duration and within the 3-day window used to estimate biological population abundance. While we developed our model in part to avoid assumptions of closure, it is not entirely possible with the survey methods used in our study; essentially, our model relaxed the assumption considerably, though did not eliminate it. Even so, given that estimates of p_p did not vary much within a year, we feel confident that we sufficiently met the closure assumption for the purpose of estimating abundance. For trend estimation, we also assumed that mean p_p was an adequate estimate of p_p in the three years with boat survey data but without telemetry data. Given that p_p varied considerably across years, this assumption likely was violated, but in the absence of annual telemetry data, we think that the mean and its associated variance are adequate because the variance was correctly incorporated into the trend variance by the Bayesian model. Also, when estimating p_k, we assumed that both murrelet species were equally likely to be classed as unidentified. We think this assumption was met reasonably well in our dataset even though Kittlitz's murrelets far outnumber marbled murrelets in our study area. Further, using field trials, we found misidentification rates of *Brachyramphus* murrelets to be low (Schaefer et al. 2015).

Our final assumption was that the tagged murrelets were representative of the biological population, as we defined it. Although our boat surveys were conducted in early July, we tagged murrelets in May because our capture technique requires darkness, which is not sufficiently available in our study area for about 6–8 weeks surrounding summer solstice (21 June). Therefore, we inevitably tagged a few birds that were transiting through Icy Bay, which we only located once or twice, or never again. These birds were not included in our estimation of p_p because they were not located during our boat surveys, so they are not relevant here. Additionally, because we only conducted telemetry flights in and near Icy Bay, it is possible that some tagged birds could have temporarily emigrated beyond our search area, which would have biased our estimation of p_p. However, we do not believe it was the case, largely because it was rare for a tagged bird to leave our study area and then return, especially as late in the breeding season as July. In fact, we removed eight locations (<2%) from our analysis because they were not within any of the five spatial states; none of those birds were located again, suggesting they permanently emigrated, or possibly the tag stopped reporting for whatever reason. Therefore, we feel confident this assumption was met as best we could with VHF transmitters.

Despite our poor ability to predict p_p, we gained new insights into the ecology of Kittlitz's murrelets. First, in previous studies of this species, we posited that, if murrelets temporarily

emigrated during boat surveys, they were moving into dense icefloes near the tidewater glaciers (i.e., Upper Bay), presumably to search for food or avoid predation (Kissling et al. 2007, Day et al. 2020). Here, we confirmed that when the proportion of ice in the Icy Bay state increased, p_p decreased, but we found that instead of moving into pack ice closer to the glacier(s), murrelets moved into shallow or rough waters away from the glaciers (i.e., East Bay and Ocean, respectively). While this finding should be viewed cautiously until confirmed at other times and locations, it appears that murrelets are less associated with ice when at sea at fine spatial scales than we previously thought, at least in the Icy Bay system.

Second, although p_p varied little within a year, it varied considerably across years, revealing a spatiotemporal pattern that implied an ecological driver(s) was at play but was not captured by the available environmental covariates. For example, p_p was comparatively low across the 15-day period in 2007 and 2010, yet in 2007, murrelets outside of the sampled area were mostly in the Ocean state and in 2010, they were mostly in the East Bay state (Appendix 3). From this result, we assume that variation in prey availability led murrelets to select states outside of the Icy Bay state, with patterns that varied on an annual, rather than a within-year, basis. With additional data from Icy Bay or elsewhere, this finding may eventually provide clues as to the ecological driver(s) of these patterns and improve our ability to predict p_p.

Our model to align statistical and biological populations for abundance estimation is simple, flexible, and scalable and is suitable for a variety of species and habitats. It is a practical solution to resolving a population mismatch when repeat and replicate sampling is not feasible and increased precision of abundance and trend estimates is desired, as is the case with many species of conservation concern like the Kittlitz's murrelet (USFWS 2013). Although it requires telemetered animals, which can be costly compared to methods for unmarked animals, it was the only reasonable way to estimate p_p for Kittlitz's murrelets in Icy Bay and we suspect the same is true for other species and habitats that are difficult to sample (e.g., walrus; Fischbach et al. 2022). The use of satellite transmitters, which are not readily available yet for murrelets, would greatly facilitate and perhaps improve estimation of p_p, especially if location data could be collected at a finer temporal scale. Moreover, satellite transmitters would relax the assumption related to representativeness of the tagged animals of the biological population and could improve precision of trend estimates if their retention and operation extended beyond a single year.

For any study reporting abundance, it is critical to clearly define the population to which abundance refers (Hammond et al. 2021), though delineating populations can be difficult and require substantial data (Rushing et al. 2016). Our goal here was not to provide a framework for how to delineate biological populations, but instead to develop an analytical approach to resolving a population mismatch if one exists. However, we urge ecologists to think critically about the population in which they want to draw inference, especially as tracking technology improves and model complexity increases. If possible, the statistical population should be the same as the biological population, or at least representative of it in terms of population processes or ecological conditions, which fortunately happened in our case. Otherwise, if p_p has temporal or geographic patterns, inference about abundance for the population of interest is confounded with its use of the sampled area and could be misleading. This messy situation with potentially misleading estimates can have conservation implications if threats or stressors vary. For

example, threatened grizzly bears (*Ursus arctos*) can roam outside of national park boundaries, with bears outside the park being subject to differing mortality sources not captured by within-park monitoring (Schwartz et al. 2010). Further, if estimates of abundance are subsequently used in population models, it is imperative that they are from the same population used to estimate other demographic parameters (e.g., survival and productivity) to avoid misleading inference about population dynamics.

AUTHORSHIP CONTRIBUTIONS

Michelle Kissling, Paul Lukacs, and Scott Gende conceived ideas and designed methodology; Michelle Kissling and Kelly Nesvacil collected the data; Michelle Kissling, Paul Lukacs, and Grey Pendleton analyzed the data; Michelle Kissling led writing of the manuscript. All authors contributed critically to drafts and gave final approval for publication.

ACKNOWLEDGEMENTS

We are grateful for the field teams in Icy Bay, 2005–2017. In particular, we acknowledge Steve Lewis, Jonathan Felis, Nick Hatch, Sarah Schoen, Joe McClung, Leah Kenney, Nick Hajdukovich, Anne Schaefer, and Jon Barton. We thank Alsek Air and Icy Bay Lodge for logistical support and Tracy Gotthardt and Bill Hanson for administrative support. We conducted this study with primary assistance from the U.S. Fish and Wildlife Service, National Park Service (Wrangell-St. Elias National Park), Alaska Department of Fish and Game (ADFG), and University of Montana. ADFG provided funding for data analysis and publication. Many thanks to Josh Schmidt, Jim Nichols, and Rebecca Taylor for helpful conversations during analysis. Scott Mills, Rob Suryan, Sarah Sells, and Josh Millspaugh provided comments on earlier drafts of this manuscript, for which we are eternally grateful. We graciously acknowledge and respect that Icy Bay and the lands that surround it are within the traditional territories of the Yakutat Tlingit Tribe.

CONFLICT OF INTEREST STATEMENT

The authors declare no conflict of interest.

DATA AVAILABILITY STATEMENT

All data collected between 2005 and 2012 that were used in this manuscript are available via Dryad at https://doi.org/10.5061/dryad.0cfxpnw8m. However, boat survey data from 2016 and 2017 were collected by the Alaska Department of Fish and Game, who considers these data to be sensitive and has withheld them in accordance with Alaska State Statute 16.05.815(d). Request of these data can be made to: Wildlife Science Director, Alaska Department of Fish and Game, Division of Wildlife Conservation, 1255 West 8th St., Juneau, Alaska, 99802 or to dfg.dwc.director@alaska.gov.

ORCID

Michelle L Kissling https://orcid.org/0000-0002-5007-584X

LITERATURE CITED

Amundson, C.L., Royle, J.A., and C.M. Handel. 2014. A hierarchical model combining distance sampling and time removal to estimate detection probability during avian point counts. The Auk 131:476–494.

Andrewartha, H.G., and L.C. Birch. 1954. The distribution and abundance of animals. University of Chicago Press, Chicago, Illinois, USA.

Barclay, D. J., J. L. Barclay, P. E . Calkin, and G. C. Wiles. 2006. A revised and extended Holocene glacial history of Icy Bay, southern Alaska, USA. Arctic, Antarctic, and Alpine Research 38: 153–162.

Barker, R.J., M.R. Schofield, W.A. Link, and J.R. Sauer. 2018. On the reliability of N-mixture models for count data. Biometrics 74:369–377.

Berryman, A.A. 2002. Population: a central concept for ecology? Oikos 97(3):439–442.

Brooks, S.P., and A. Gelman. 1998. General methods for monitoring convergence of iterative simulations. Journal of Computational and Graphical Statistics 7:434–455.

Buckland, S.T., D.R. Anderson, K.P. Burnham, J.L. Laake, D.L. Borchers, and L. Thomas. 2001. Introduction to distance sampling. Oxford University Press, Oxford, United Kingdom.

Burnham, K.P., D.R. Anderson, G.C. White, C. Brownie, K.H. Pollock. 1987. Design and analysis methods for fish survival experiments based on release-recapture. American Fisheries Society Monograph 5, Bethesda, Maryland, USA.

Camus, P.A., and M. Lima. 2002. Populations, metapopulations, and the open-closed dilemma: the conflict between operational and natural population concepts. Oikos 97(3):433–438.

Chandler, R.B., J.A. Royle, and D.I. King. 2011. Inference about density and temporary emigration in unmarked populations. Ecology 92:1429–1435.

Cochran, W.G. 1977. Sampling techniques. John Wiley and Sons, New York, New York, USA.

Day, R. H., M.L. Kissling, K J. Kuletz, D.A. Nigro, and P. Pyle. 2020. Kittlitz's Murrelet (*Brachyramphus brevirostris*), version 1.0. In Birds of the World (P. G. Rodewald, Editor). Cornell Lab of Ornithology, Ithaca, NY, USA. https://doi.org/10.2173/bow.kitmur.01

Fischbach, A.S., R.L. Taylor, C.V. Jay. 2022. Regional walrus abundance estimate in the United States Chukchi Sea in autumn. Journal of Wildlife Management 86:e22256. https://doi.org/10.1002/jwmg.22256

Hammond, P.S., T.B. Francis, D. Heinemann, K.J. Long, J.E. Moore, A.E. Punt, R.R. Reeves, M. Sepulveda, G.M. Sigurosson, M.C. Siple, G. Vikingsson, P.R. Wade, R. Williams, and A.N. Zerbini. 2021. Estimating the abundance of marine mammal populations. Frontiers in Marine Science 8:735770. doi: 10.3389/fmars.2021.735770

Hoekman, S. T. 2019. Kittlitz's murrelet monitoring in Glacier Bay National Park and Preserve 2010–2018: Synthesis and program review. Natural Resource Report NPS/SEAN/NRR—2019/1957. National Park Service, Fort Collins, Colorado, USA.

Hostetter, N.J., B. Gardner, T.S. Sillett, K.H. Pollock, and T.R. Simons. 2019. An integrated model decomposing the components of detection probability and abundance in unmarked populations. Ecosphere 10(3), Article e02586.

Kendall, W.L., J.D. Nichols, and J.E. Hines. 1997. Estimating temporary emigration using capture-recapture data with Pollock's robust design. Ecology 78:563–578.

Kery, M., and J.A. Royle. 2016. Applied hierarchical modeling in ecology. Academic Press, San Diego, California, USA.

Kissling, M.L. 2023. Linking life history and population dynamics of an ice-associated seabird, the Kittlitz's murrelet (*Brachyramphus brevirostris*). PhD dissertation, University of Montana, Missoula, USA.

Kissling, M.L., S.M. Gende, S.B. Lewis, and P.M. Lukacs. 2015a. Reproductive performance of Kittlitz's Murrelet in a glaciated landscape, Icy Bay, Alaska. The Condor: Ornithological Applications 117:237–248.

Kissling, M.L., P.M. Lukacs, S.M. Gende, and S.B. Lewis. 2015b. Multi-state mark-recapture model to estimate survival of a dispersed-nesting seabird, the Kittlitz's murrelet. Journal of Wildlife Management 79:20–30.

Kissling, M.L., P.M. Lukacs, S.B. Lewis, S.M. Gende, K.J. Kuletz, N.R. Hatch, S.K. Schoen, and S. Oehlers. 2011. Distribution and abundance of the Kittlitz's Murrelet *Brachyramphus brevirostris* in selected areas of southeastern Alaska. Marine Ornithology 39:3–11.

Kissling, M.L., M. Reid, P.M. Lukacs, S.M. Gende, and S.B. Lewis. 2007. Understanding abundance patterns of a declining seabird: implications for monitoring. Ecological Applications 17:2164–2174.

Lukacs, P.M., M.L. Kissling, M. Reid, S.M. Gende, and S.B. Lewis. 2010. Testing assumptions of distance sampling of a pelagic seabird. Condor 112(3):455–459.

Mizel, J.D., J.H. Schmidt, and M.S. Lindberg. 2018. Accommodating temporary emigration in spatial distance sampling models. Journal of Applied Ecology 55:1456–1464. https://doi.org/10.1111/1365-2664.13053

Newman, S.H., J.Y. Takekawa, D.L. Whitworth, and E. Burkett. 1999. Subcutaneous anchor attachment increases retention of radio transmitters on seabirds: Xantus' and Marbled murrelets. Journal of Field Ornithology 70:520–534.

728 Nichols, J.D., L. Thomas, and P.B. Conn. 2009. Inferences about landbird abundance from count
729 data: recent advances and future directions. Pages 201–235 *In* Modeling demographic processes
730 in marked populations (D.L. Thompson, E.G. Cooch, and M.J. Conroy, Editors). Springer, New
731 York, USA.
732
733 National Oceanic and Atmospheric Administration (NOAA). 2007. Observers guide to sea ice.
734 Emergency Response Division, National Ice Center, Seattle, Washington. Available online:
735 https://response.restoration.noaa.gov/oil-and-chemical-spills/oil-spills/resources/observers-
736 guide-sea-ice.html
737
738 Plummer, M. 2003. JAGS: A program for analysis of Bayesian graphical models using Gibbs
739 sampling. Proceedings of the 3rd International Workshop on Distributed Statistical Computing,
740 March, 20–22, 2003, Vienna, Austria.
741
742 R Core Team. 2019. R: a language and environment for statistical computing. R Foundation for
743 Statistical Computing, Vienna, Austria.
744
745 Reynolds, J.H. 2012. An overview of statistical considerations in long-term monitoring. *In*
746 Design and Analysis of Long-term Ecological Monitoring Studies (R.A. Gitzen, J.J. Millspaugh,
747 A.B. Cooper, and D.S. Licht, editors). Cambridge University Press, Cambridge, United
748 Kingdom.
749
750 Royle, J.A. 2004. *N*-mixture models for estimating population size from spatially replicated
751 counts. Biometrics 60:108–115.
752
753 Royle, J.A., & Dorazio, R. M. 2008. Hierarchical modeling and inference in ecology. Academic
754 Press, London, United Kingdom.
755
756 Royle, J.A., and K.V. Young. 2008. A hierarchical model for spatial capture-recapture data.
757 Ecology 89:2281–2289.
758
759 Rushing, C.S., T.B. Ryder, A.L. Scarpignato, J.F. Saracco, and P.P. Marra. 2016. Using
760 demographic attributes from long-term monitoring data to delineate natural population structure.
761 Journal of Applied Ecology 53:491–500.
762
763 Schaefer, A.M., P.M. Lukacs, and M.L. Kissling. 2015. Testing factors influencing the detection
764 rates of similar species during abundance surveys. The Condor: Ornithological Applications
765 117:460–472.
766
767 Schaub, M., O. Gimenez, A. Sierro, and R. Arlettaz. 2007. Use of integrated modeling to
768 enhance estimates of population dynamics obtained from limited data. Conservation Biology
769 21:945–955.
770
771 Schwartz, C.C., M.A. Haroldson, and G.C. White. 2010. Hazards affecting grizzly bear survival
772 in the Greater Yellowstone Ecosystem. Journal of Wildlife Management 74:654–667.
773

774 Schwarz, C.J., and A.N. Arnason. 1996. A general methodology for the analysis of capture-
775 recapture experiments in open populations. Biometrics 52:860–873.
776
777 U.S. Fish and Wildlife Service (USFWS). 2013. 12-month finding on a petition to list Kittlitz's
778 Murrelet as an endangered or threatened species. Federal Register 78:61764.
779
780 Waples, R.S., and O. Gaggiotti. 2006. What is a population? An empirical evaluation of some
781 genetic methods for identifying the number of gene pools and their degree of connectivity.
782 Molecular Ecology 15:1419–1439.
783
784 White, G.C. and R.A. Garrott. 1990. Analysis of wildlife radio-tracking data. Academic Press,
785 New York, New York, USA.
786
787 Whitworth, D.L., J.Y. Takekawa, H.R. Carter, and W.R. McIver. 1997. A night-lighting
788 technique for at-sea capture of Xantus' Murrelets. Colonial Waterbirds 20:525–531.
789
790 Wisdom, M.J., L.S. Mills, and D.F. Doak. 2000. Life stage simulation analysis: estimating vital-
791 rate effects on population growth for conservation. Ecology 81:628–641.

Table 1. Sample sizes and effort by survey type for estimating abundance of a biological population of Kittlitz's murrelets, Icy Bay, Alaska, 1–15 July 2005–2017. Truncation distance was used to model the detection function to estimate probability of detection (p_d) with distance sampling data.

Year	Boat surveys				Telemetry surveys		
	# surveys	Portion of sampling area surveyed		Truncation distance (m)	15-day period		
		Survey 1	Survey 2		# flights	# radio-tagged individuals	# locations
2005	2	0.85	0.85	250	-	-	-
2007	2	0.75	0.74	281	4	24	82
2008	2	0.75	0.70	278	8	20	137
2009[a]	1	0.91	-	288	5	20	85
2010	2	0.67	0.91	242	3	24	58
2011	2	0.77	0.73	210	4	27	100
2012	2	0.75	0.56	181	4	17	54
2016	2	0.91	1.00	325	-	-	-
2017	2	0.91	0.90	323	-	-	-

[a]Boat survey conducted on 17 July 2009; telemetry survey information presented here for 1–15 July 2009.

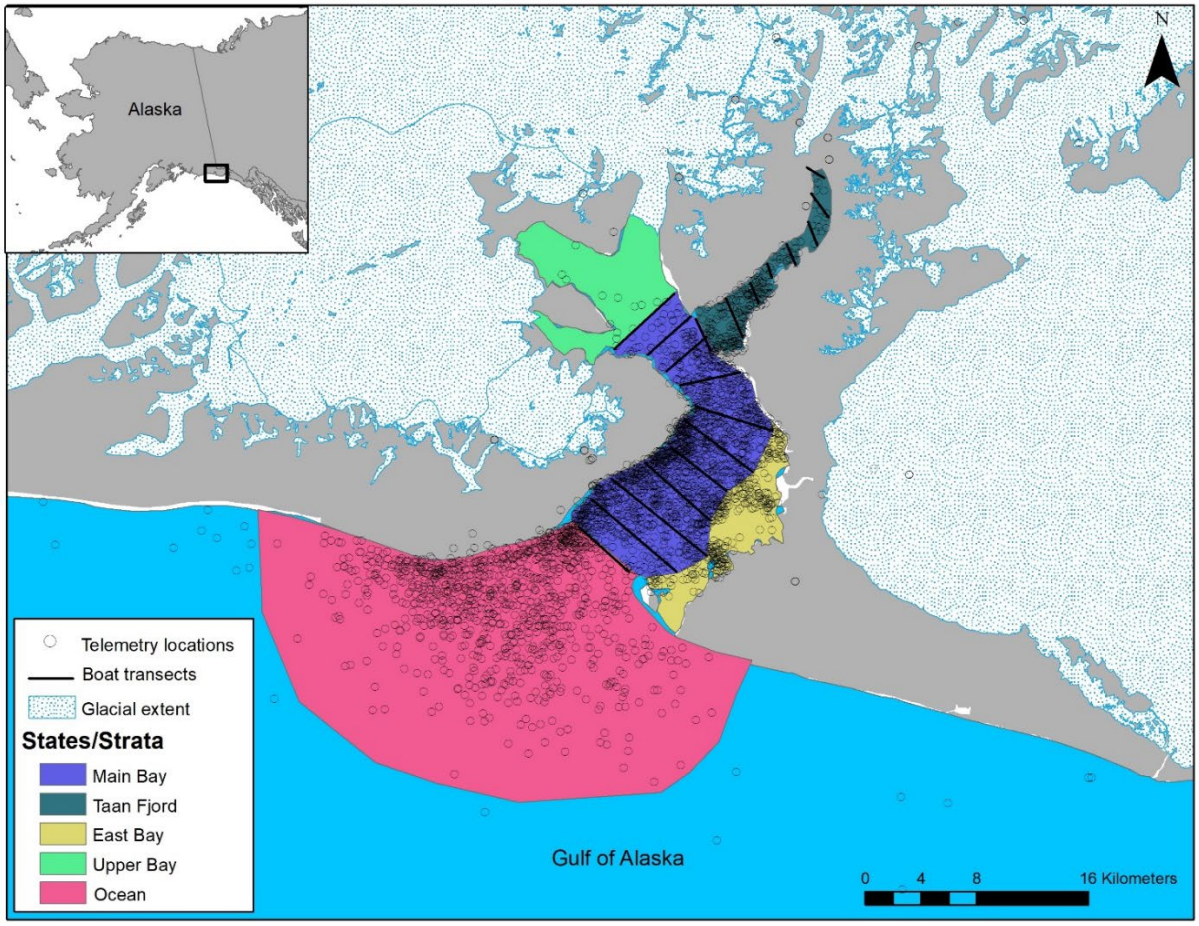

Figure 1. Map of study area, Icy Bay, Alaska, where we conducted boat and telemetry surveys to estimate abundance of Kittlitz's murrelets. Our sampling area during telemetry flights comprised five spatial states that collectively formed the extent of the biological population: Icy Bay (Main Bay and Taan Fjord sub-states combined), East Bay, Upper Bay, Ocean, and nest. During boat surveys, only the Icy Bay state, with Main Bay and Taan Fjord as strata, was regularly accessible and formed the extent of the statistical population.

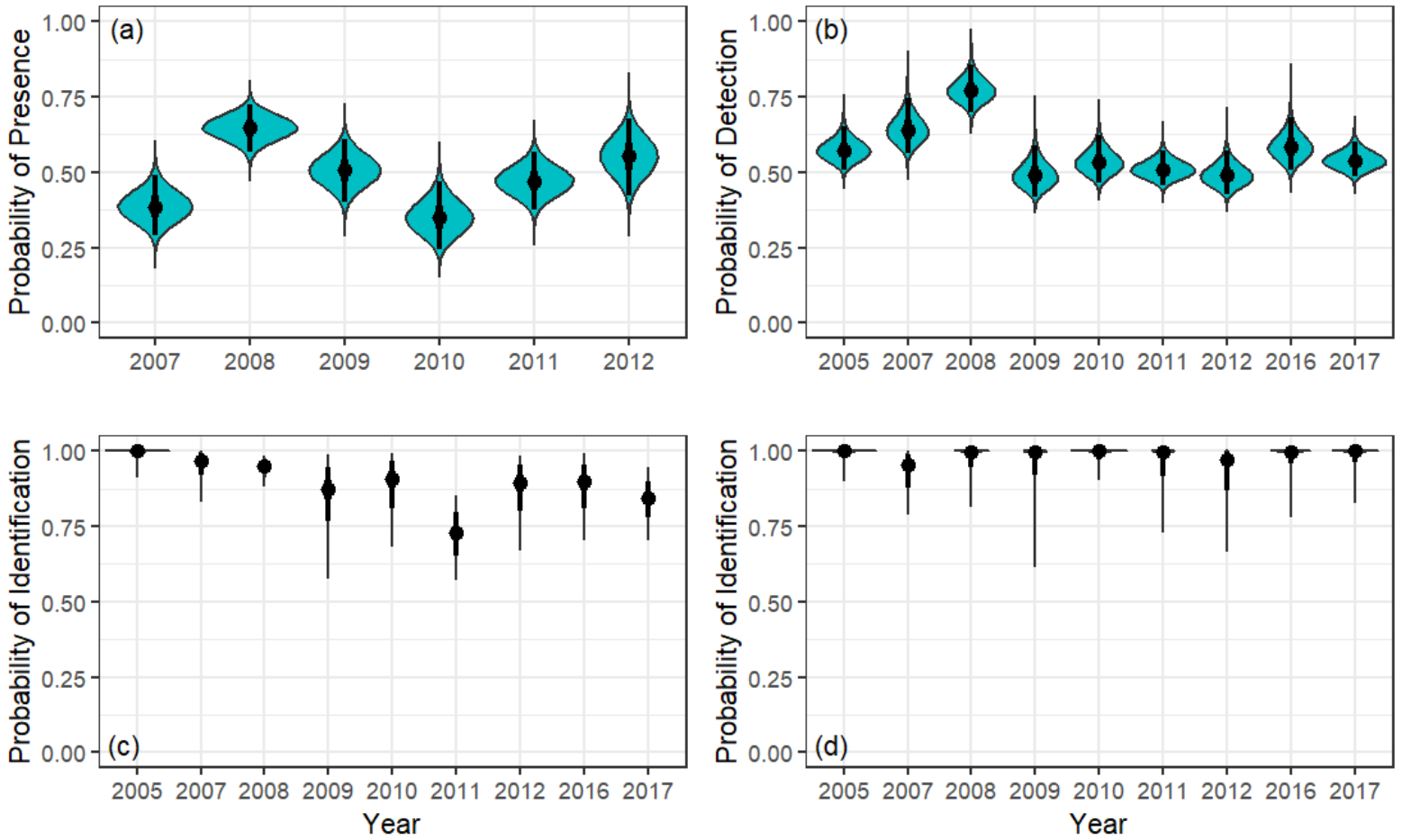

Figure 2. Posterior distributions of estimates of detection probability components for Kittlitz's murrelets, Icy Bay, Alaska, 2005–2017. Components are (a) probability of presence (p_p), (b) probability of detection (p_d), and probability of being a Kittlitz's murrelet (p_k) in (c) Main Bay and (d) Taan Fjord strata. The median of the estimate is denoted with a point, the 50% credible interval with a thick line, and the 95% credible interval with a thin line. Note that for p_d (b), truncation distance varied across years (Table 1).

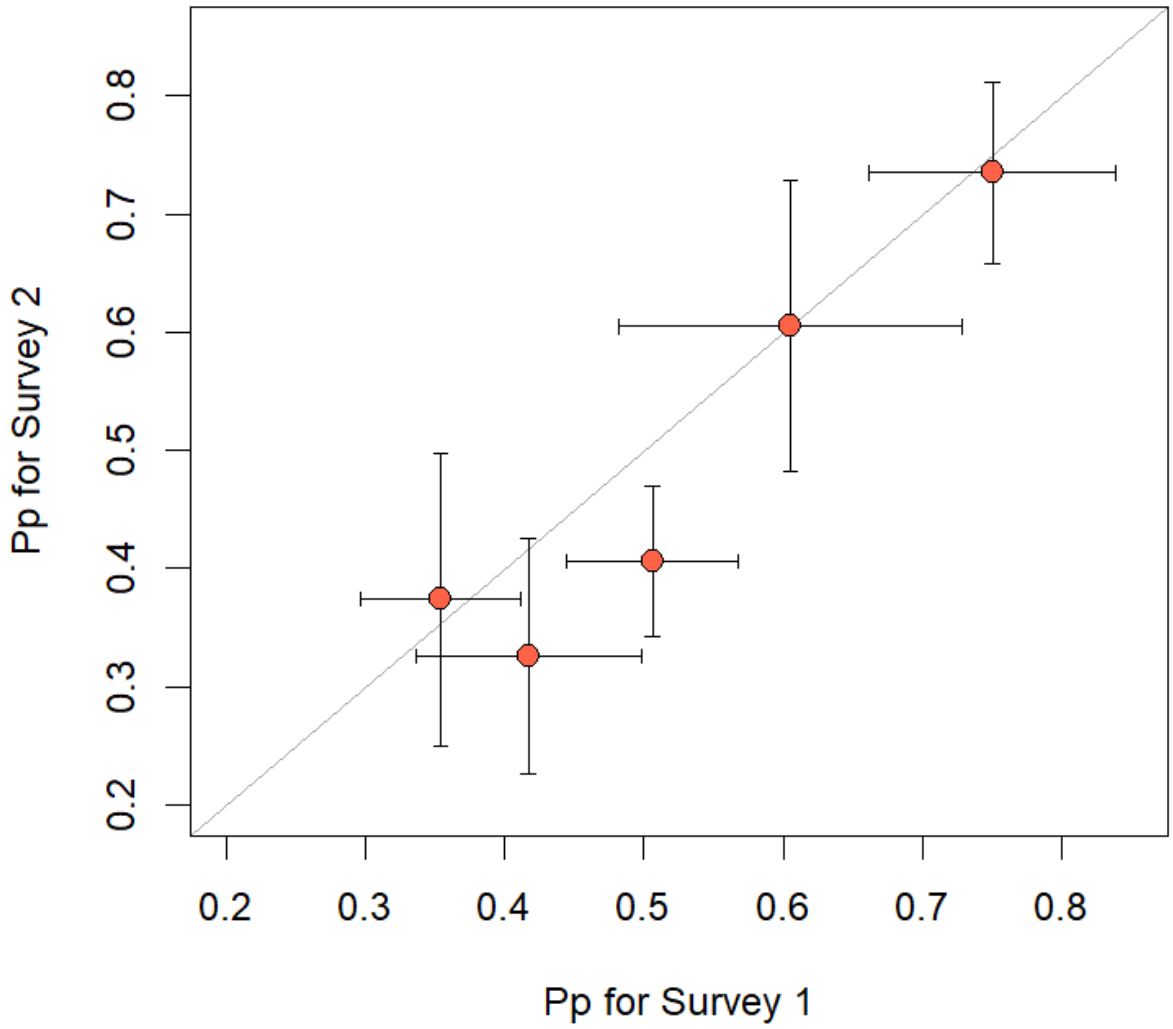

Figure 3. Probability of presence (p_p) for the 3-day window by boat survey within a year. The error bars describe the standard errors of the estimate and correspond with the respective axes. The identity, or 1:1 line, is included in gray.

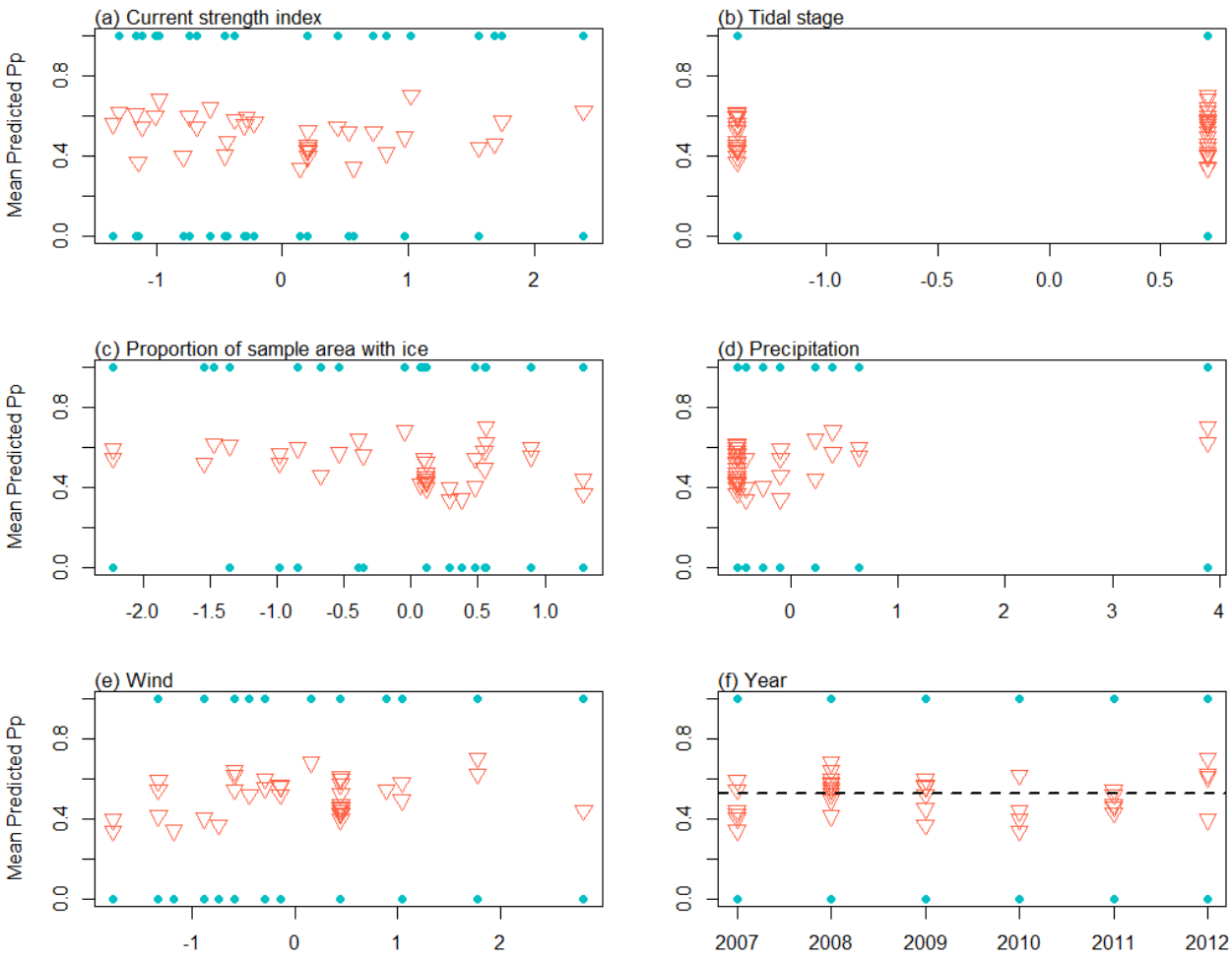

Figure 4. Observed outcomes (teal points) and predicted probability of presence (p_p; orange triangles) using environmental covariates for Kittlitz's murrelets, Icy Bay Alaska, 2007– 2012. Covariates on x-axis are scaled; see 'Methods' text for description. For year (f), the dotted line denotes the mean p_p across all years in the observed dataset.

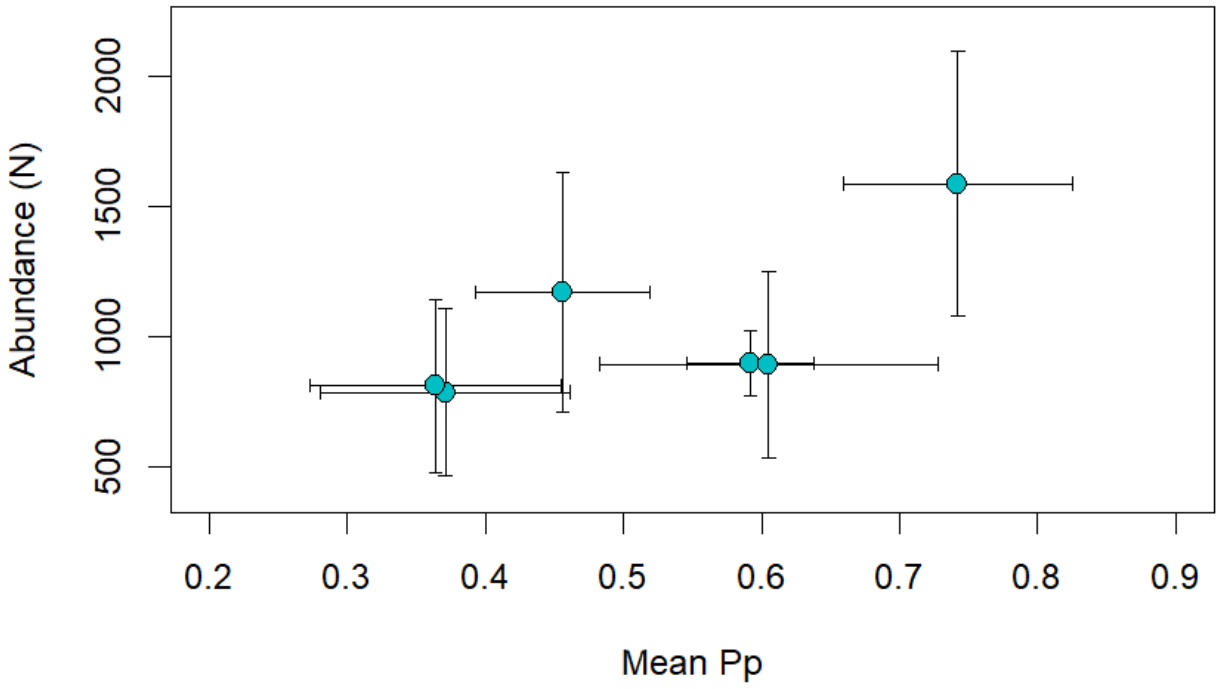

Figure 5. Mean probability of presence (p_p) across both surveys for the 3-day window by abundance of the statistical population, i.e., without p_p. The error bars describe the standard errors of the estimate and correspond with the axes.

Figure 6. Posterior distributions of annual abundances estimate for the Kittlitz's murrelet and corresponding coefficients of variation (triangles) without probability of presence (p_p; statistical population) and with p_p (3-day window; biological population) around corresponding boat surveys, Icy Bay, Alaska. In 2009, when only one boat survey was completed, the posterior distribution was extremely narrow (overly precise) and extends beyond the y-axis limits of this figure for display purposes.

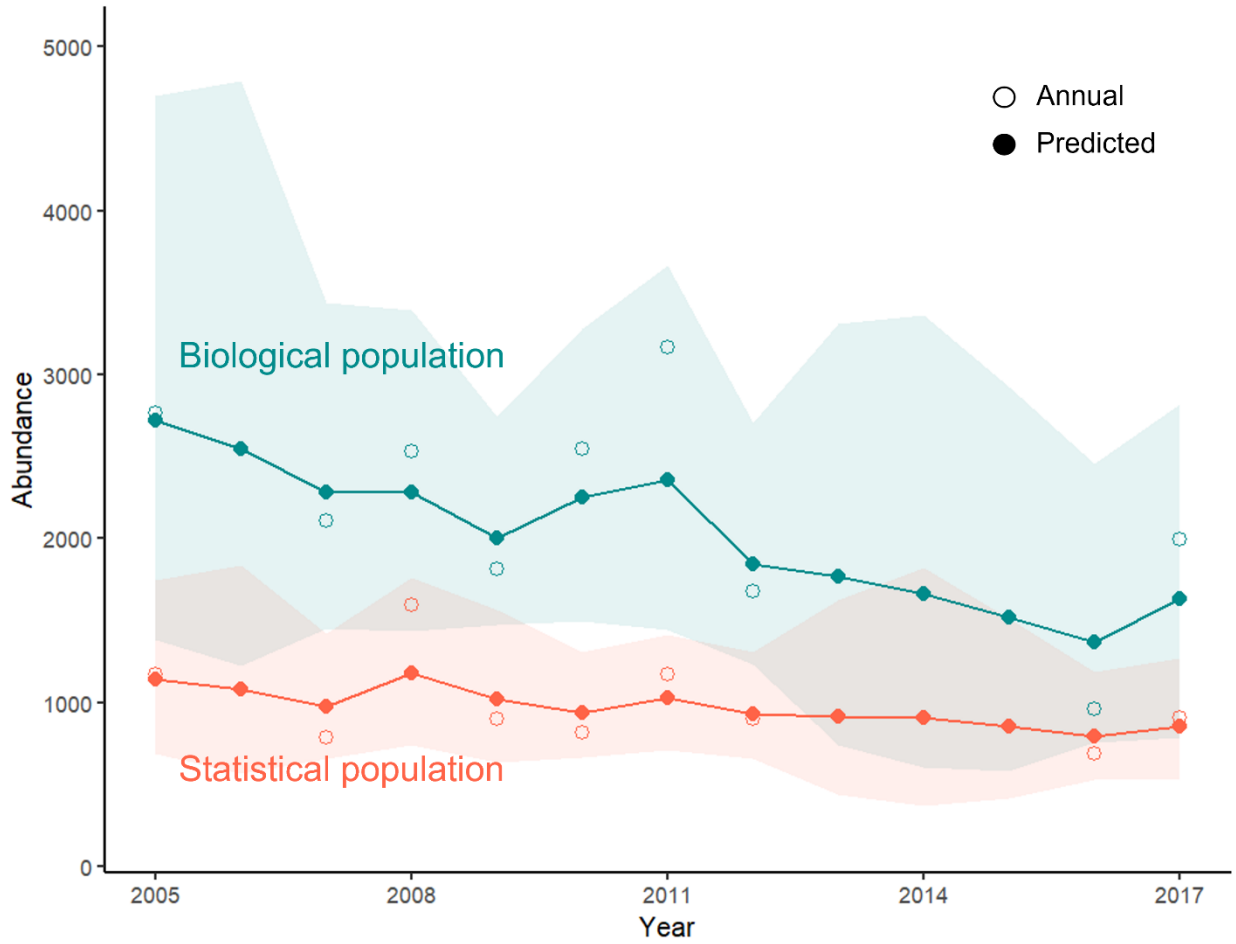

Figure 7. Annual and predicted abundance estimates of the statistical population (without probability of presence, p_p) and biological population (with p_p) of Kittlitz's murrelets, Icy Bay, Alaska, 2005–2017. Annual estimates are denoted with open circles and predicted estimates from the state-space model are identified with closed circles; the shaded areas describe the 95% credible intervals of the modeled abundance. P_p is accounted for in the biological population estimates using telemetry data surrounding a 3-day window of a boat survey.

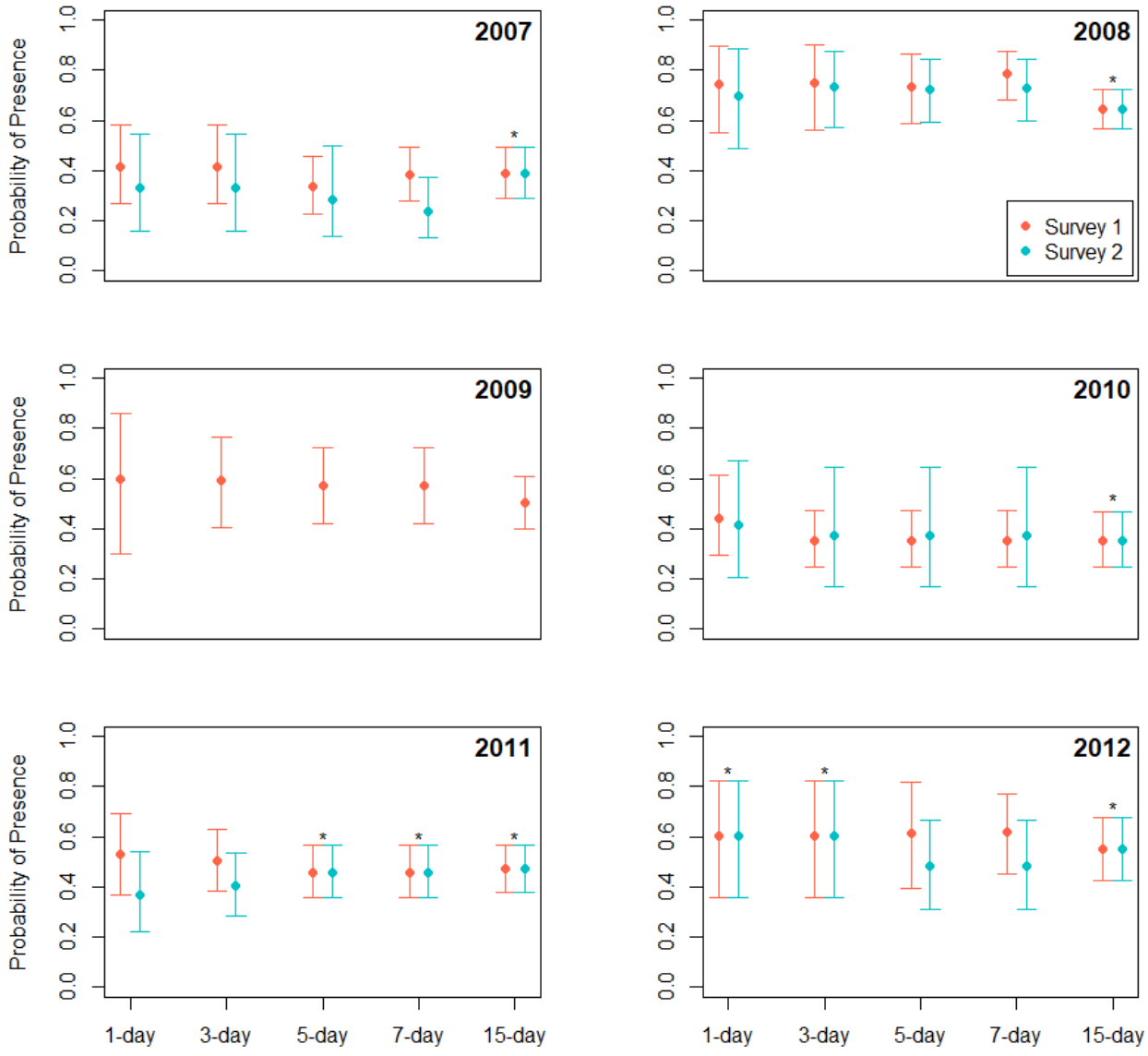

Appendix 1. Estimates of probability of presence (p_p; ± 95% credible intervals) of radio-tagged Kittlitz's murrelets by window length (1-, 3-, 5-, 7-day, and 15-day) and boat survey (survey 1=black, survey 2=red), Icy Bay, Alaska, 1–15 July 2007–2012. Asterisks indicate windows when the same telemetry data were used to estimate p_p for boat surveys 1 and 2.

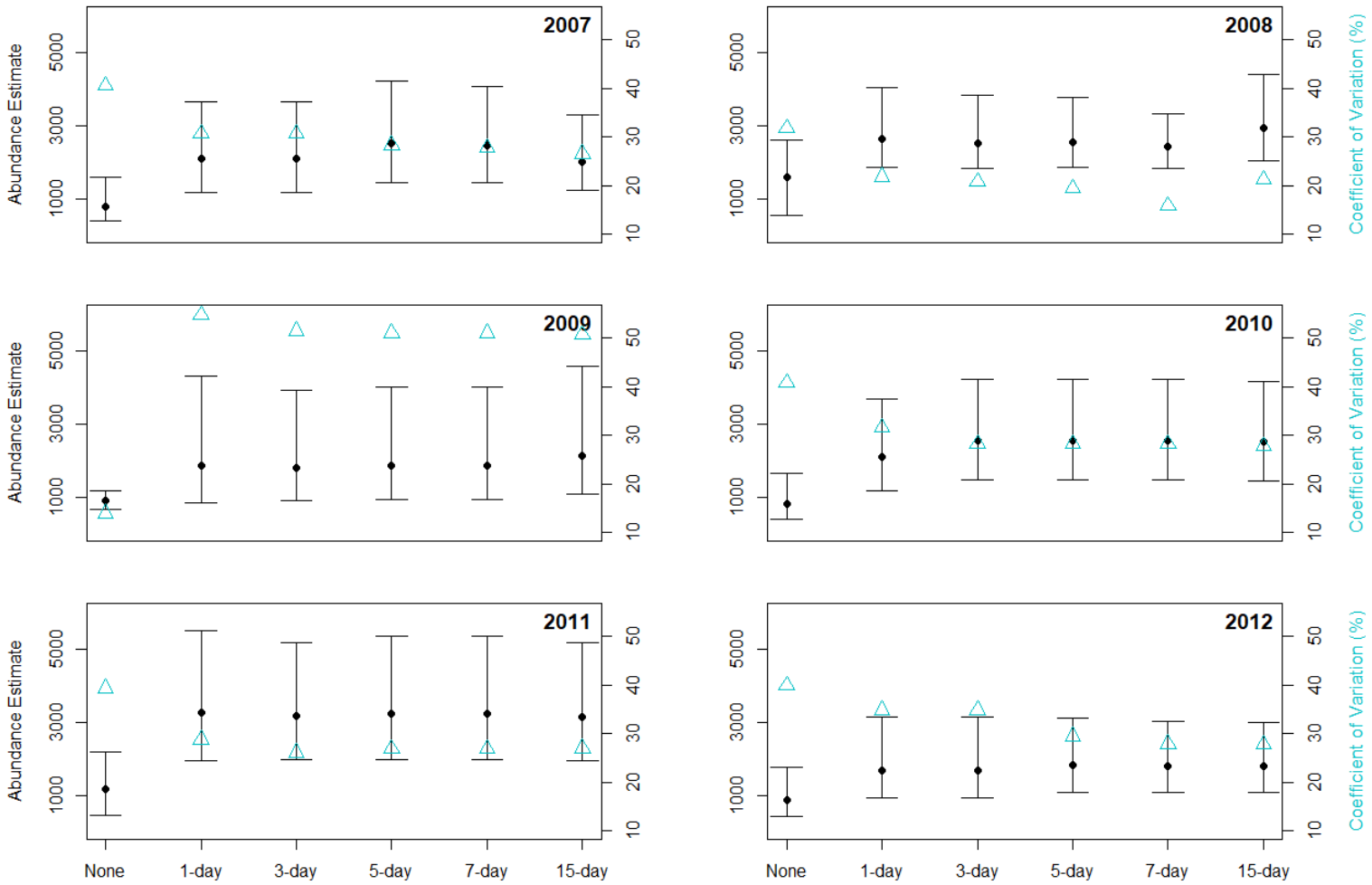

Appendix 2. Kittlitz's murrelet annual abundance estimates and 95% credible intervals (black) and corresponding coefficients of variation (blue) without probability of presence (p_p; None; statistical population) and with p_p by window length (1-, 3-, 5-, and 7-day; biological population) around corresponding boat surveys and entire window (15-day) when boat surveys were conducted (i.e. 1–15 July), Icy Bay, Alaska. We completed two boat surveys each year except 2009 when only one survey was done.

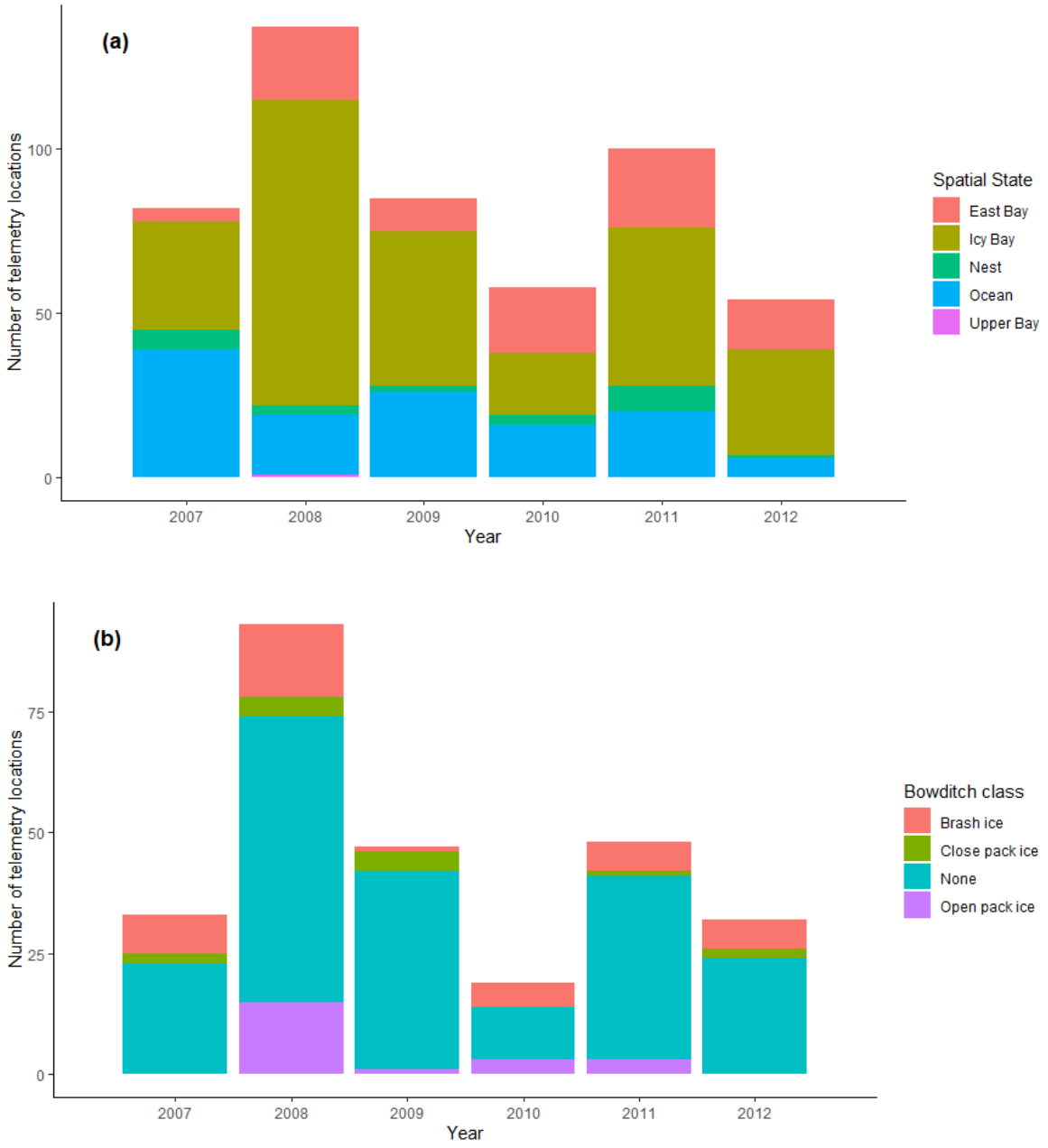

Appendix 3. Number of telemetry locations of Kittlitz's murrelets by year and (a) spatial state and (b) Bowditch ice class, 1–15 July 2007–2012, Icy Bay, Alaska. We did not location any murrelets in very close pack ice.

Appendix 4. JAGS code and priors
All raw data and code are included in data release via Dryad at:
https://doi.org/10.5061/dryad.0cfxpnw8m

integrated model for abundance with prob of presence from telemetry data, probability of detection from distance sampling data, and probability of being a Kittlitz's murrelet to allocated unidentified murrelets in JAGS for two boat surveys in a year

```
model {
  ##### priors
  ### priors for distance sampling, group size, and speciesID
  # data augmentation parameter; proportion of z's that are real animals
  for( i in 1:nstrata){
   psi1[i] ~ dunif(0,1)   # in survey 1
   psi2[i] ~ dunif(0,1)   # in survey 2
  }

  # intercept for probability of being KIMU
  for( i in 1:nstrata){
   b0.sid[i] ~ dnorm( 0, 0.01 ) T(-10,10)
   logit(mean.sid1[i]) <- b0.sid[i]
   logit(mean.sid2[i]) <- b0.sid[i]
  }

  lambda.group ~ dunif(1, 10)     # dgamma(0.1, 0.1)    # prior for group size
  alpha0 ~ dunif(-10, 10)       # intercept for sigma (shape of detection function)
  #alpha1 ~ dunif(-10, 10)     # prior for group size effect on detection function (if using)

  ### priors for prob of being in core area
  #beta0 ~ dnorm( 0, 0.01 )T(-10,10)  # prior for intercept (if needed)
  beta1 ~ dnorm( 0, 0.01 )T(-10,10)  # prior for Survey1
  beta2 ~ dnorm( 0, 0.01 )T(-10,10)  # prior for Survey2

  ##### likelihood
  ### likelihood for distance sampling, group size, and speciesID for survey 1
  for ( m in 1:nstrata) {

  for( i in 1:nind.dist1){

   # process model
   z1[i,m] ~ dbern(psi1[m])    # fake and real animals
   x1[i,m] ~ dunif(0, B)   # distribution of distances; B is max distance of strip width
   species.id1[i,m] ~ dbern( mean.sid1[m])    # prob of being a KIMU
   group.size1[i,m] ~ dpois(lambda.group)  # distribution of group size

   # observation model
```

```
  # log(sigma1[i,m]) <- alpha0 + alpha1 * group.size1[i,m]   # if using group size
  log(sigma1[i,m]) <- alpha0  # if not using group size in detection function
  logdp1[i,m] <- -((x1[i,m]*x1[i,m]) / (2*sigma1[i,m]*sigma1[i,m]))     # half normal
  dp1[i,m] <- exp(logdp1[i,m])
  mu1[i,m] <- z1[i,m] * dp1[i,m]
  y1[i,m] ~ dbern( mu1[i,m] )   # likelihood for probability of detection (pd; distance sampling)

  zg1[i,m] <- z1[i,m] * (group.size1[i,m] )   # number of individuals in group i
}

}

### likelihood for distance sampling, group size, and speciesID for survey 2
for (m in 1:nstrata) {

for( i in 1:nind.dist2){

  # process model
  z2[i,m] ~ dbern(psi2[m])
  x2[i,m] ~ dunif(0, B)
  species.id2[i,m] ~ dbern( mean.sid2[m])
  group.size2[i,m] ~ dpois(lambda.group)

  # observation model
  # log(sigma2[i,m]) <- alpha0 + alpha1 * group.size2[i,m]
  log(sigma2[i,m]) <- alpha0
  logdp2[i,m] <- -((x2[i,m]*x2[i,m]) / (2*sigma2[i,m]*sigma2[i,m]))
  dp2[i,m] <- exp(logdp2[i,m])
  mu2[i,m] <- z2[i,m] * dp2[i,m]
  y2[i,m] ~ dbern( mu2[i,m] )

  zg2[i,m] <- z2[i,m] * (group.size2[i,m] )
}

}

### likelihood for prob of being in core area
# for survey 1
for( i in 1:nlocs1 ) {
 core1[i] ~ dbern(p1[i])    # likelihood for probability of presence (pp)
 logit(p1[i]) <- beta1      # success probability
}

# for survey 2
for( i in 1:nlocs2 ) {
 core2[i] ~ dbern(p2[i])
```

```
 logit(p2[i]) <- beta2
}

##### derived parameters
### derived parameters for distance sampling, group size, and speciesID
G[1] <- sum(z1[,1])
G[2] <- sum(z1[,2])
G[3] <- sum(z2[,1])
G[4] <- sum(z2[,2])

### population size of KIMU (study area km2 / (transect length * strip width))
# population size of KIMU in MB for survey 1
N.1[1] <- sum(zg1[1:nind.dist1, 1] * species.id1[1:nind.dist1, 1])
   * (mb1.km2 / (mb.length1 * (B*2/1000)))

# population size of KIMU in TF for survey 1
N.1[2] <- sum(zg1[1:nind.dist1, 2] * species.id1[1:nind.dist1, 2])
   * (tf1.km2 / (tf.length1 * (B*2/1000)))

# estimated population size of KIMU for survey 1
N[1] <- sum(N.1[1], N.1[2])

# population size of KIMU in MB for survey 2
N.2[1] <- sum(zg2[1:nind.dist2, 1] * species.id2[1:nind.dist2, 1])
   * (mb2.km2 / (mb.length2 * (B*2/1000)))

# population size of KIMU in TF for survey 2
N.2[2] <- sum(zg2[1:nind.dist2, 2] * species.id2[1:nind.dist2, 2])
   * (tf2.km2 / (tf.length2 * (B*2/1000)))

# estimated population size of KIMU for survey 2
N[2] <- sum(N.2[1], N.2[2])

### derived parameters for prob of being in core area
# mean prob of presence in core area for survey 1
logit(core.p[1]) <- beta1

# mean prob of presence in core area for survey 2
logit(core.p[2]) <- beta2

### integrated model for abundance of biological population
# prior for Ntot
logNtot ~ dunif(6, 10)

Ntot <- exp(logNtot)
sigmaN <- Ntot*core.p[1]*(1-core.p[1])    # approximate SE
```

```
   for( m in 1:nsurvey){
     muN[m] <- exp( -( ((N[m]/core.p[m])-Ntot)*((N[m]/core.p[m])-Ntot  )) /
(2*sigmaN*sigmaN) )
     yN[m] ~ dbern(muN[m])
   }
  }

##### state space model to estimate trend in abundance of murrelets with random effects for
year and weighted response variable (log abundance) by inverse of the variance in JAGS

model {
  ##### priors
  logN.pred[1] ~ dnorm(7, 0.01)   # initial population size

  mean.r ~ dnorm(0, 0.001)   # mean growth rate

  sigma.r ~ dunif(0, 1)   # SD of state process
  tau.r <- pow(sigma.r, -2)

  sigma.obs ~ dunif(0, 1)   # SD of observation process
  tau.obs <- pow(sigma.obs, -2)

  mean.y ~ dunif(0, 3000)
  tau.y ~ dunif(0, 50)

  for (t in 1:nyears){
  y[t] ~ dnorm(mean.y, tau.y) T(0, 10000)
  }

  mean.sd ~ dunif(0, 1000)
  tau.sd ~ dunif(0, 10)

  for (t in 1:nyears){
  y.sd[t] ~ dnorm(mean.sd, tau.sd) T(0, 2000)
  }

  ##### likelihood
  ## state process
  for (t in 1:(nyears-1)){
    r[t] ~ dnorm(mean.r, tau.r)
    logN.pred[t+1] <- logN.pred[t] + r[t]
  }

  ## observation process
```

```
  for (t in 1:nyears){
    logy[t] ~ dnorm(logN.pred[t], tau.obs*(y.sd[t]/y[t])^2)
  }

  ## derived parameter - population size on real scale
  for (t in 1:nyears){
    N.pred[t] <- exp(logN.pred[t])
  }

}
```